

WEATHERING OF BASALT: FORMATION OF IDDINGSITE

KATHERINE L. SMITH,¹ ANTHONY R. MILNES,² AND RICHARD A. EGGLETON³

¹ Department of Physics, New South Wales Institute of Technology
Sydney, New South Wales, Australia

² CSIRO Division of Soils
Glen Osmond, South Australia, Australia

³ Department of Geology, Australian National University
G.P.O. Box 4, Canberra City 2601, Australia

Abstract—The formation of iddingsite by the oxidative weathering of Fo₈₀ olivine begins by solution of Mg from planar fissures, 20 Å wide and spaced 200 Å apart, parallel to (001). Oxidation of Fe within the remaining olivine provides nuclei for the topotactic growth of goethite. Cleavage cracks <50 Å in diameter allow Na, Al, and Ca from adjacent minerals, particularly plagioclase, to enter the altering olivine while Mg and Si diffuse away. In the early stages of weathering, strips of Fe-rich smectite (saponite), 20–50 Å wide and 1–7 layers thick, form bridges 50–100 Å long across the planar fissures. Dioctahedral smectite crystallizes on the margins of wider cleavage-controlled fissures; with further weathering halloysite is formed away from the fissure walls. In the ultimate stages of alteration, the saponite and dioctahedral smectite are lost, leaving a porous, oriented aggregate of goethite crystals each measuring about 50 × 100 × 200 Å (X, Y, Z, respectively), with sporadic veins of halloysite crossing the pseudomorph.

Key Words—Goethite, Iddingsite, Iron, Olivine, Scanning electron microscopy, Transmission electron microscopy, Weathering.

INTRODUCTION

Olivine is a most reactive mineral both under hydrothermal conditions and during weathering. Many mineral assemblages, grouped under the “omnibus” terms iddingsite or bowlingite (Deer *et al.*, 1962; Delvigne *et al.*, 1979), comprise the weathering products of olivine. Bowlingite in thin section looks “to be a micaceous fine-grained aggregate in which individual flakes are usually randomly distributed” (Delvigne *et al.*, 1979). It is regarded as an olivine alteration product formed under non-oxidative conditions (Wilshire, 1958). When the weathering environment becomes oxidizing, bowlingite is itself altered to a complex mixture containing goethite and kaolin. The weathering of olivine via bowlingite will be reported in a later paper.

Iddingsite is composed of a mixture of goethite and smectite in which the X-, Y-, and Z-axes of the goethite and the Z-, X-, and Y-axes of the clay are parallel to the X-, Y-, and Z-axes of olivine. These crystallographic relationships suggest that iddingsite nucleates epitactically or topotactically on its parent olivine (Brown and Stephen, 1959; Gay and Le Maitre, 1961; Eggleton, 1984). During weathering, the formation of iddingsite is generally initiated at the margins of olivine crystals (Delvigne *et al.*, 1979). It appears to invade the crystals progressively until, in the most extensively altered samples, the original olivine is entirely transformed. Iddingsite is reddish orange in color and, viewed between crossed polars, extinguishes parallel to the extinction direction of the olivine. It may be regarded as the product of oxidative weathering of olivine (Colman, 1982).

Eggleton *et al.* (1987) described the bulk chemical and mineralogical changes that take place during weathering of basalt corestones *in situ*. Subsequent studies have been concerned with the weathering of individual basalt minerals. In this paper we report on investigations of the formation of iddingsite using optical microscopy, electron probe microanalysis (EPMA), scanning electron microscopy (SEM), high-resolution transmission electron microscopy (HRTEM), selected-area diffraction (SAD), and analytical electron microscopy (AEM). Samples of the basalts examined were from Limberg (Sasbach, Federal Republic of Germany), Baynton (Victoria, Australia), and Townsville (Queensland, Australia). It will be demonstrated that the model proposed for the alteration of the Limberg olivine to iddingsite by Eggleton (1984) is equally applicable to the alteration of these other olivines.

TECHNIQUES

For optical microscope studies, polished thin sections were prepared of weathered basalt samples impregnated with synthetic resins. EPMA of olivine and its alteration zones and products identified optically in these polished thin sections were made using a Technisch Physisch Dienst energy-dispersive X-ray (EDX) system at the Research School of Earth Sciences (Australian National University) and a Cambridge Instruments ‘Geoscan’ wavelength-dispersive X-ray system at CSIRO Division of Soils.

For SEM, altered olivine crystals were carefully handpicked from weathered basalt samples, mounted on aluminum stubs, and sputter coated with carbon.

Table 1. Electron probe microanalyses of iddingsites.

	B0 Olivine	B1 Iddingsite	B7 Iddingsite	T0 Olivine	T1 Iddingsite	T2 Iddingsite	T3 Iddingsite
SiO ₂	39.57	37.65	27.24	37.5	33.4	14.62	4.83
Al ₂ O ₃	—	1.81	1.99	0.07	0.71	9.16	7.66
FeO	17.05	31.41	42.01				
Fe ₂ O ₃				22.5	30.8	49.0	67.1
MnO	0.10	0.19	0.20	n.d.	n.d.	0.12	n.d.
MgO	42.90	21.91	20.28	40.1	26.5	5.55	0.24
CaO	0.17	0.65	0.30	0.26	0.46	0.29	n.d.
K ₂ O		0.23			0.02		n.d.
TiO ₂				0.03	0.06	0.22	0.65
Na ₂ O				0.04	0.70	1.25	0.55
Total	99.79	93.85	92.02	100.5	92.7	80.2	81.0

B = Baynton, Victoria; T = Townsville, Queensland; n.d. = not determined.

These samples were examined in a Cambridge Stereoscan 250 Mk 3.

Specimens for TEM, HRTEM, and AEM investigations were prepared by ion-bombardment thinning of selected areas of polished thin sections that contained altered olivine crystals in suitable orientation. The brass grids used to support specimens generally encircled other minerals besides olivine, and therefore particular care was taken to locate features observed in the TEM accurately relative to photomicrographs taken of the specimen before and after ion-bombardment thinning. Extensive areas of iddingsite were accessible in all ion-beam thinned TEM specimens of altered olivines, and there appears to have been little difference in the thinning rates of olivine and iddingsite.

The microstructure of the olivines was studied in JEOL 100CX and JEOL 200CX transmission electron microscopes operated at 100 and 200 kV, respectively. Chemical analyses of the Baynton and Limberg olivines were obtained at 100 kV using a JEOL 200CX instrument equipped with an ASID scanning device, an energy-dispersive X-ray detector, and PGT data-collection equipment. PGT data-reduction software was used to strip spectra of their backgrounds and to integrate peaks. Analyses of the Townsville basalt minerals were obtained using a Philips 430 electron microscope equipped with a Tracor-Northern energy-dispersive

X-ray detector and data-processing system. Within each spectrum, ratios were calculated of the integrated peak heights of individual elements to the integrated peak height of Si. The correction factors for AEM data depend critically on specimen thickness. For analyses obtained on the Philips instrument, the factors to convert integrated peak heights to atomic proportions relative to Si are Mg: 2.1; Al: 1.2; and Fe: 0.6, providing the specimen is extremely thin (100–500 Å). A comparison of EPMA and AEM analyses of olivine and goethite (Tables 1 and 2) indicates that AEM analyses for Mg: Si are correct to within 10% of the amount present, but that the Fe:Si ratio may be overestimated in thicker areas.

SAMPLES

The Limberg olivine was described by Eggleton (1984). Most crystals have iddingsite rims which are thought to have been formed by alteration prior to weathering. The Baynton basalt contains fresh olivine (Fo₈₂), plagioclase (An₅₅), and augite set in a glass peppered with magnetite and ilmenite inclusions. The weathering of this basalt was described by Wilson (1978) and Eggleton *et al.* (1987). From the centers of the basalt corestones to the outer weathered rinds, the olivine crystals are progressively altered to produce pseudomorphs of red-brown iddingsite.

The samples studied most comprehensively during this investigation were from Townsville (Queensland), and were collected across a weathered corestone of alkali basalt. In the center of the corestone, basalt samples are comparatively fresh and contain unaltered olivine that displays the variable formation of iddingsite in zones around the margins of the crystals. Plagioclase (An₅₅₋₆₀), augite, and pigeonite are the other dominant minerals. Ilmenite and magnetite are conspicuous as fine-grained, opaque crystals mainly associated with the pyroxenes. In samples from the weathered rind of the corestone, olivine crystals are completely pseudomorphed by iddingsite. The other major minerals pres-

Table 2. Element ratios in altered olivines from Townsville.¹

	Mg	Al	Si	Ca	Fe
a. Olivine	1.5	0	1.0	0	0.5
b. Diamond textured	1.2	0	1.0	0	0.7
c. Clay in lamellae	1.0	0	1.0	0	0.7
d. Channel smectite	0.0	0.30	1.0	0.05	0.30
e. Halloysite	0.0	0.8	1.0	0	0.2
f. Goethite	0	0.15	0.04	0	0.85
g. Goethite ²	0	0.17	0.08	0	0.83

¹ Analytical electron microscopic data.

² Electron microprobe data.

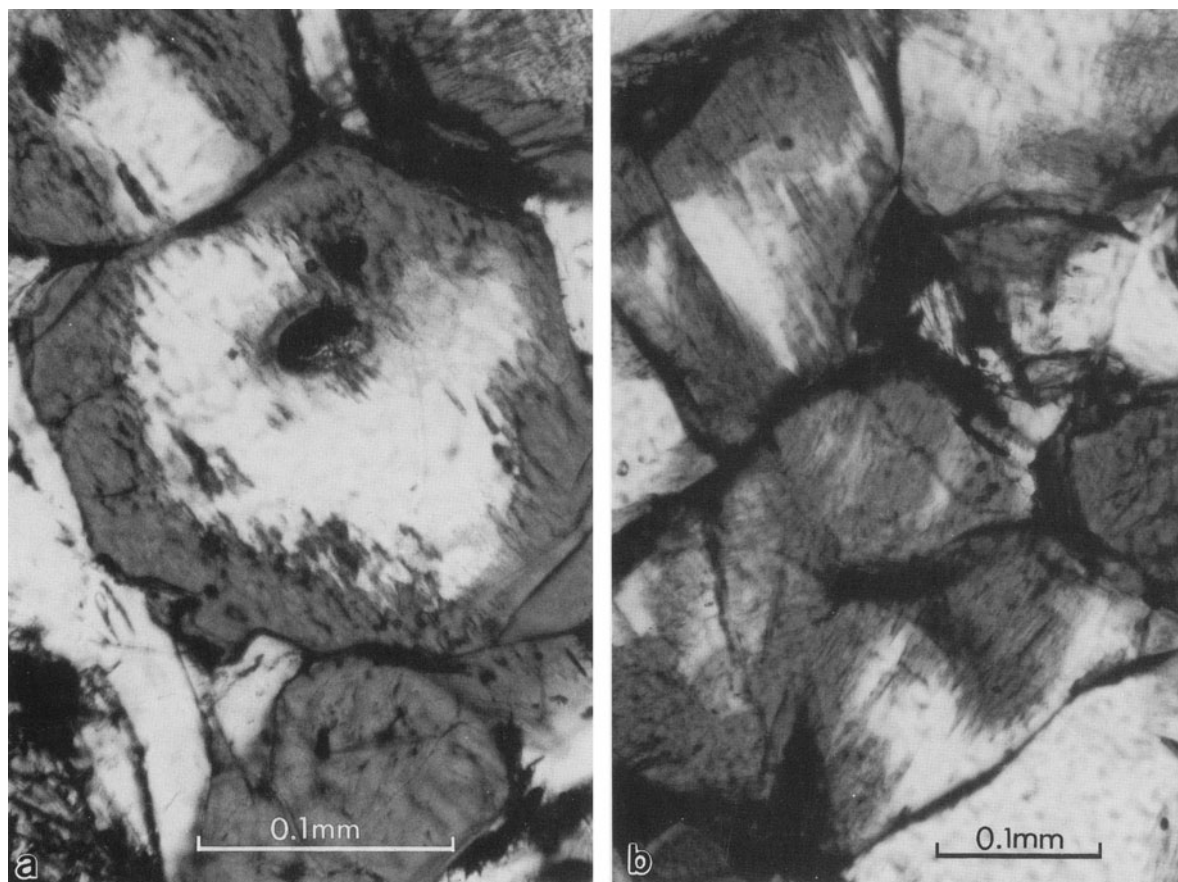


Figure 1. (a) Photomicrograph of olivine (Fo_{80}) showing alteration rim of brown iddingsite; sample M422 from center of Townsville basalt corestone. Unaltered olivine, clear. Inner margins of alteration rims characterized by linear structure due to penetration of alteration phases along fissures oriented parallel to (001). Pale coloration at alteration boundary due to phyllosilicate phase. Clear crystals marginal to olivine are plagioclase (An_{50}). Height of field, 0.35 mm. Transmitted plane polarized light. (b) Photomicrograph showing cluster of olivine crystals partly altered to iddingsite; Townsville basalt sample M422. Unaltered olivine, clear. Note well-developed channels parallel to (001), along which alteration consists initially of pale-colored clay merging into darker iddingsite. Width of field, 0.35 mm. Transmitted plane polarized light.

ent (based on X-ray powder diffraction (XRD) data for whole samples) are kaolinite and halloysite.

RESULTS

Optics

Clues to the weathering processes resulting in the ultimate transformation of olivine to iddingsite were readily obtained from optical studies of polished thin sections of the weathered basalts. Alteration of olivine proceeds via the ingression of planar fissures or channels filled with microcrystalline alteration products from the margins of the crystals or from internal cleavage planes or fractures (Figures 1 and 2). The channels are parallel to (001) and are responsible for the typical lamellar structure in partly altered olivine grains. In detail, the channels are wedge-shaped, with the sharp points of the wedges projecting into the unaltered olivine (Figure 1b). Initial stages of weathering are char-

acterized by pale yellow-brown material in the frontal zones of the advancing wedge-shaped channels (Figures 1 and 2). The bulk of the alteration zones which rim the partly transformed crystals, however, is composed of red-brown to orange colored material (Figure 1). The optical characteristics of the alteration zones, particularly birefringence, indicate a mixture of phases, including microcrystalline clay. In samples in which the weathering of olivine is essentially complete, goethite was identified from optical properties as the dominant product.

Chemistry

EPMA of the optically identified weathering features of olivine crystals in polished thin sections of the Baynton and Townsville basalt are summarized in Table 1 and Figures 3 and 4. Degradation of the iddingsite under the influence of the focused beam during analysis caused problems when the wavelength-dispersive mi-

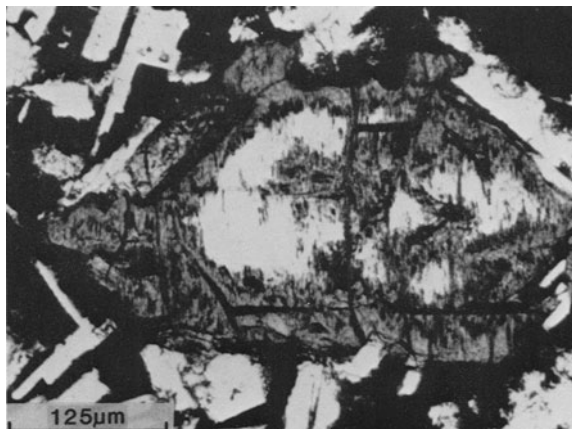


Figure 2. Photomicrograph of Baynton olivine viewed parallel to *X*, showing alteration to iddingsite extending along (001) from crystal margins and from (010) cleavages.

croprobe was used. With a stationary beam, increases in Fe counts ranging from 5 to 18% were experienced over the 30-s counting time, although the resulting totals for the analyses approached the theoretical value for goethite ($\text{Fe}_2\text{O}_3 = 89.8\%$). Stable conditions showing no discernible change in count rate with time were obtained by moving the focused beam during the analysis. The analyses under these circumstances gave variably low totals, as low as 55%. Element ratios, however, were unaffected by the analytical conditions. These data indicate that the iddingsite pseudomorphs are variably hydrated, and that water is probably lost due to the combined effect of heating and photochemical degradation. Our experience is that many goethite samples are pseudomorphous after olivine, but not all are de-

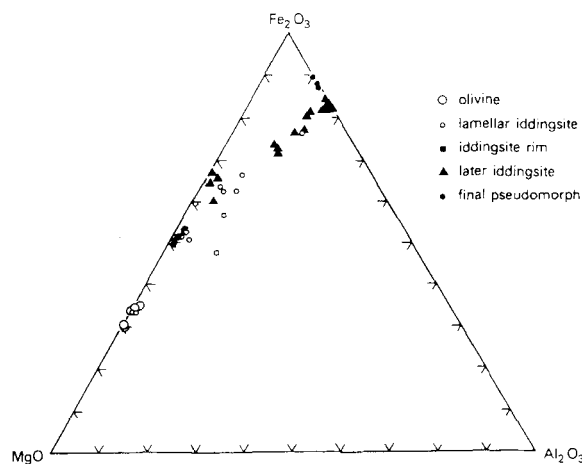


Figure 3. Triangular composition diagram for components Fe_2O_3 , Al_2O_3 , and MgO showing uniform change in chemical composition (electron microprobe data) of alteration products of Townsville olivine with progressive weathering of host basalt.

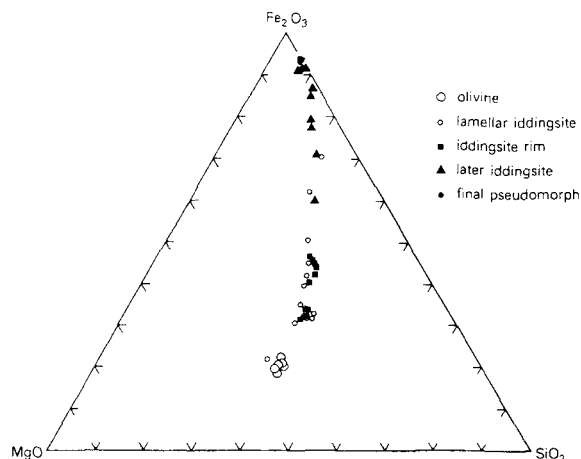


Figure 4. Triangular composition diagram for components Fe_2O_3 , SiO_2 , and MgO showing uniform change in chemical composition (electron microprobe) of alteration products of Townsville olivine with progressive weathering of host basalt.

graded by the electron beam during EPMA. On the other hand, examples of well-crystallized goethite from localities including the Restormel mine in Cornwall, United Kingdom, and the Superior mine in Michigan are not affected.

Compared with unaltered olivine crystals, the various stages of weathering encompass a progressive gain of Fe, Al, and Ti and a concomitant loss of Mg and Si (Table 1; Figures 3 and 4). The initial products contain variable amounts of Al, which is absent from the parent olivine, in combination with Si, Mg, and Fe derived from the olivine. These materials are probably smectitic clays admixed with goethite. The later products are Fe-rich, containing moderate concentrations of Al (as much as about 10% Al_2O_3 absolute) and Si ($\text{Al}:\text{Si} \cong 2.2$), but contain little Mg. The ultimate product is dominantly goethite containing somewhat less Al and Si (Figures 3 and 4). The presence of a clay mineral phase is indicated from the Al and Si concentrations, but some Al substitutes in the goethite structure; it is also possible that all of the Al and Si are substituted in the goethite. No definitive diffraction data have been obtained to distinguish between these possibilities.

X-ray scanning images (Figure 5) show the distribution of particular elements in the marginal zones of olivines exhibiting early stages of weathering. Al is concentrated in fractures which lead inwards from the margins of the crystals; it is also enriched in distinctive lamellar-structured zones adjacent to the fractures. Fe is similarly enriched in these zones, whereas Mg and Si (image not included in Figure 5) are depleted. Na is also enriched in parts of the lamellar-structured zones, but its distribution can not be strictly correlated with that of either Fe or Al. A distinct rim can be recognized on some weathered olivine crystals (e.g., Figure 5),

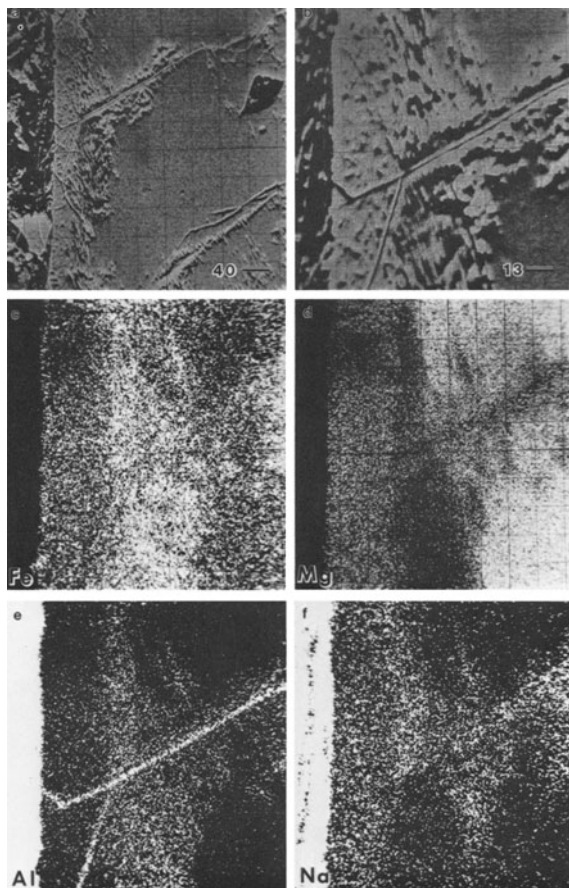


Figure 5. Images of Townsville olivine and lamellar-structured alteration zones of iddingsite in polished thin sections. (a), (b) Backscattered electron images. (c)–(f) X-ray scanning images for Fe, Mg, Al, and Na. Lamellar zones adjacent to cleavage fractures seen in (a) and (b) are depleted in Mg and enriched in Fe and Al. Na is concentrated in some parts of these zones, but is not directly correlated with Fe and Al. Al is clearly concentrated in fractures leading into olivine from adjacent plagioclase (Al-, Na-rich region at left). Scale bar in micrometers.

which is enriched in Mg, Si, and Na, but depleted in Fe relative to the lamellar zones.

Scanning electron microscopy

SEM studies of the Townsville samples provide detailed observational data. The lamellar zone of weathering between unaltered olivine and one of the Al-enriched fractures identified from X-ray scanning images (Figure 5) is shown in Figure 6. The lamellar zone is characterized by planar discontinuities in which irregularly distributed tabular bodies are generally $< 2 \mu\text{m}$ in length. EDX analyses indicate that these masses are enriched in Al compared with the adjacent olivine; they are accordingly regarded as accumulations of clay minerals. The adjacent fracture is covered by hemispherical masses (about $0.3 \mu\text{m}$ in diameter) clustered together to form a mammillary coating, which was also

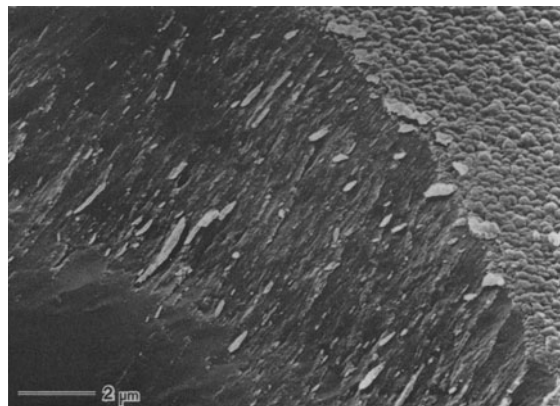


Figure 6. Scanning electron micrograph of lamellar zone of altered olivine in Townsville basalt sample M422. Unaltered olivine, bottom left; lamellar zone (center) composed of planar structures along which alteration has produced an irregular array of tabular clay masses (light-colored ridges). At top right, mammillary coating of hemispherical masses of clay (halloysite), each about $0.3 \mu\text{m}$ diameter, on cleavage fracture surface immediately adjacent to lamellar zone.

identified from EDX analyses as essentially clay. Such material occurs extensively on fracture surfaces in olivine in the early stages of weathering (Figure 7) and is likely to be halloysite based on XRD data for bulk samples of basalt.

Completely iddingsitized olivine crystals composed dominantly of goethite are shown in Figure 8. Minor concentrations of Al, Si, and Ti are evident from EDX analyses, confirming EPMA data obtained for the same crystals in polished thin sections. Etched lamellar-structured zones conspicuous in parts of the pseudomorph may represent modifications of the clay-filled features which characterize the initial stages of weathering of olivine crystals.

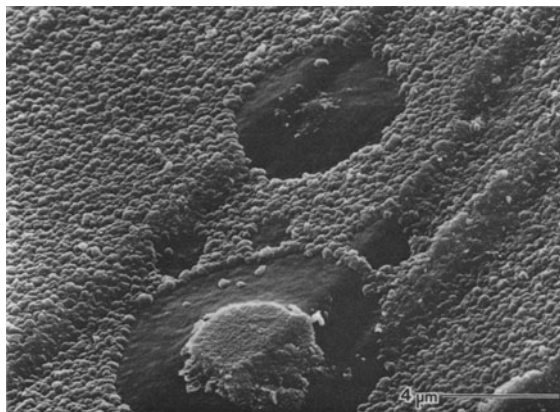


Figure 7. Scanning electron micrograph of cleavage or fracture surface in olivine (sample M422) with hemispherical masses of clay (halloysite) clustered together to form mammillary coating on apparently unaltered olivine.

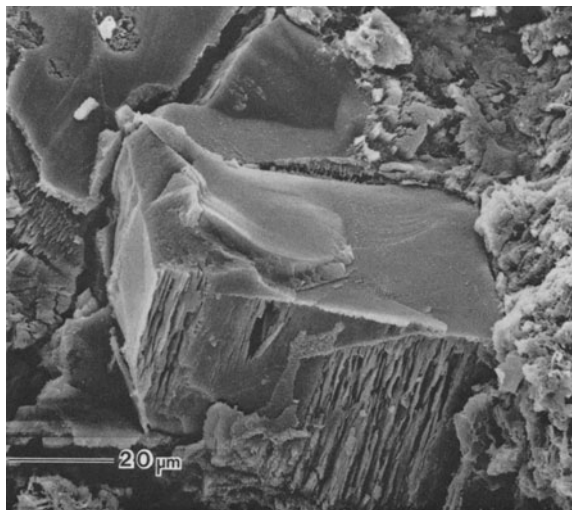


Figure 8. Scanning electron micrograph of completely iddingsitized olivine crystal in Townsville basalt sample M427. Optical characteristics together with energy-dispersive X-ray and electron microprobe data for this material indicate mainly goethite. Note conspicuous etched lamellar zones at front of crystal. Sample matrix on right dominantly kaolinite.

Transmission electron microscopy

Iddingsite formation on a TEM scale was first described by Eggleton (1984). The following discussion expands and modifies his model using observations made on iddingsite from Baynton and Townsville. With regard to the initial stages of weathering, sections of olivine viewed perpendicular to the Z -axis reveal the above-mentioned lamellar-structured zone as a region of planar fissures developed parallel to (001), as shown in Figure 9. The spacing between the planar fissures or channels is always about 200 \AA . In some samples, strips of phyllosilicate $<50 \text{ \AA}$ wide bridge the fissures at approximately regular intervals (Figure 10). From the composite SAD pattern of olivine and clay at this stage of alteration of the Limberg sample, Eggleton (1984) reported that the Z -, Y -, and X -axes of the clay were parallel to the X -, Y -, and Z -axes of the olivine, re-

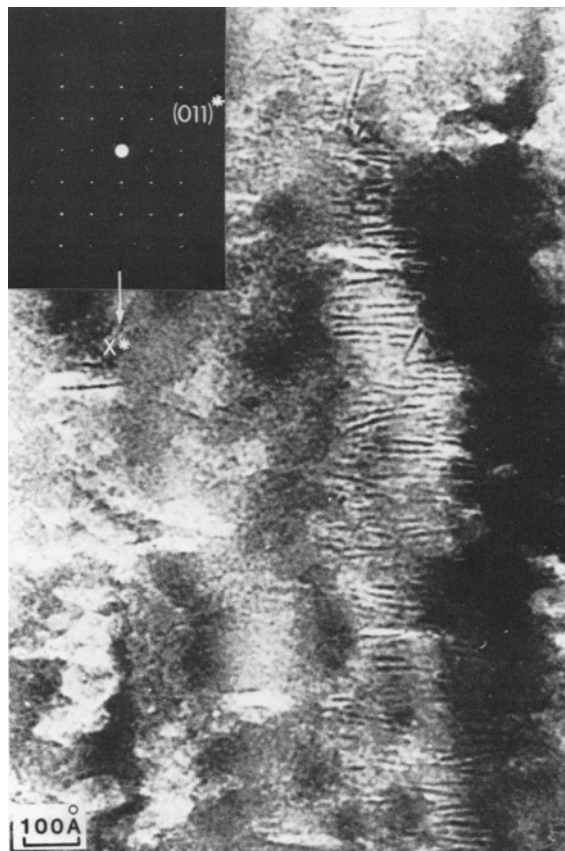


Figure 10. Transmission electron micrograph showing strips of phyllosilicate crossing an etch lamella. Early stages of Townsville olivine alteration; view parallel to $[0\bar{1}1]$.

spectively. In all three olivines investigated in the present study, the bridging layer silicate was so sensitive to the electron beam that it was not possible to photograph its lattice image. In confirmation of the data obtained from EPMA analyses of the lamellar-structured zones, AEM data indicate a loss of Mg relative to that in unaltered olivine (Figure 11; Table 2, analysis c).

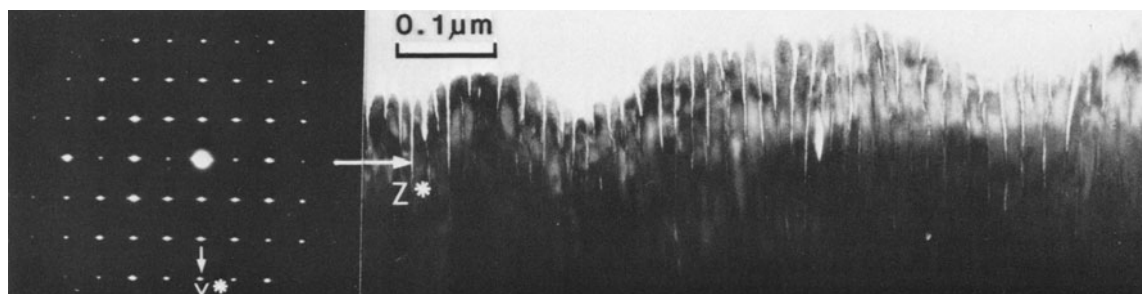


Figure 9. Transmission electron micrograph of lamellar iddingsite (Townsville) showing parallel etch channels spaced about 200 \AA apart.

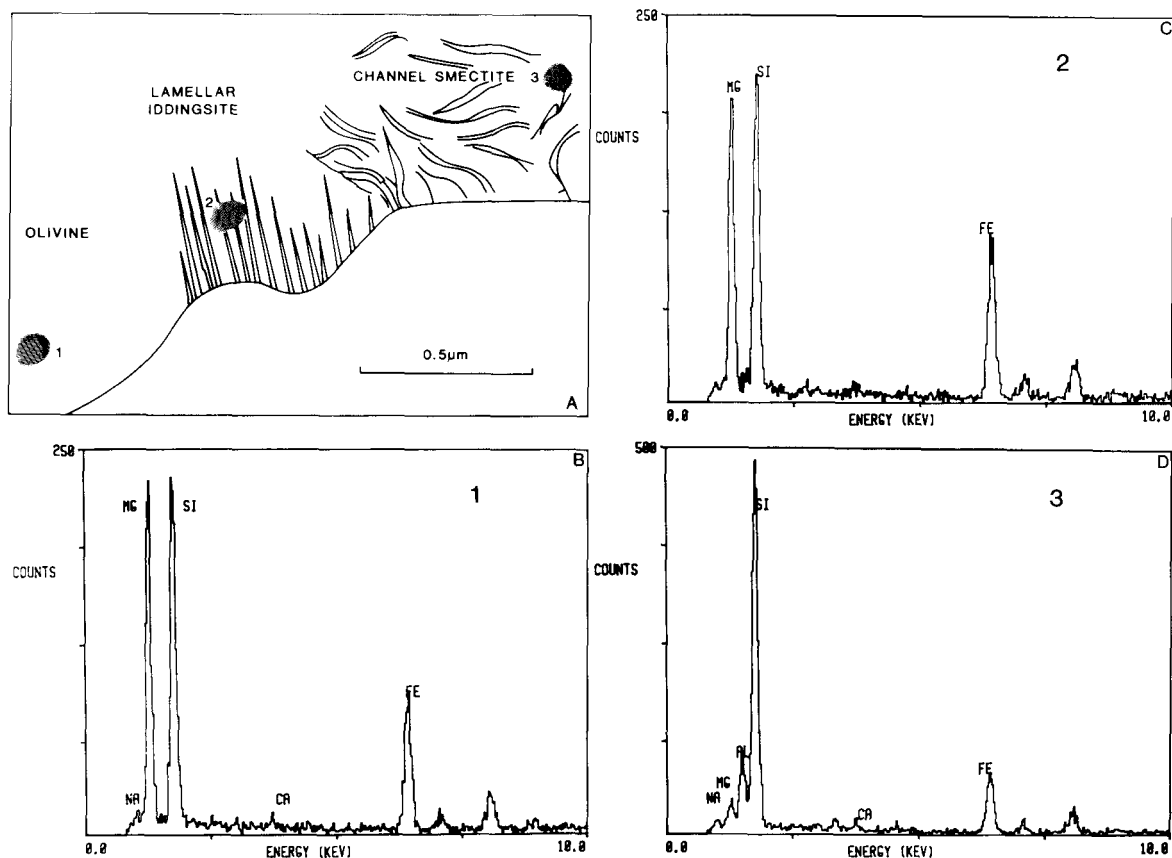


Figure 11. Analytical electron microscopic results for Limburg olivine and iddingsite. (A) drawing of region analyzed; (B) olivine analysis (area 1); (C) analysis of lamellar iddingsite (area 2); (D) analysis of channel clay (area 3). Note the loss of Mg and increase in Al from (1) to (3).

In the Limberg sample, large channel structures contain clay bridges which are longer along their Z-axis and wider along their Y-axis. Long wisps of clay in the wider gaps bear no orientation relationship to the olivine (Eggleton, 1984). Figure 11 shows a drawing of a typical area of Limberg olivine that grades from fresh olivine to randomly oriented clay. AEM X-ray spectra taken at the positions of the numbered spots are also illustrated, and the corresponding data are given in Table 2. The composition of areas of lamellar structure are little different from that of the unaltered olivine, whereas the clay in large channels contains much less Mg and Fe, appreciable Al, and usually identifiable concentrations of Ca. This clay is much more stable in the electron beam than that present in the fissures of the lamellar-structured zones, and high-resolution images show 10-Å lattice spacings and some larger basal spacings, as high as 11.5 Å.

Many types of fabric are visible if iddingsite is viewed in the [001] section. As described by Eggleton (1984) for the Limberg olivine, the first evidence of alteration is the breakdown of olivine into a mosaic of diamond-shaped domains, each about 50 Å long and bounded

by {110}. This stage is followed by the formation of a 10-Å phyllosilicate having (001) parallel or subparallel to (001) of the olivine. In the Townsville olivine, more-altered regions contain small, electron-dense, diamond-shaped crystallites (Figure 12) shown by AEM to be Fe-rich (Table 2, analysis f). This fact, combined with the similarity of these crystallites to the microstructures Smith and Eggleton (1983) observed on a

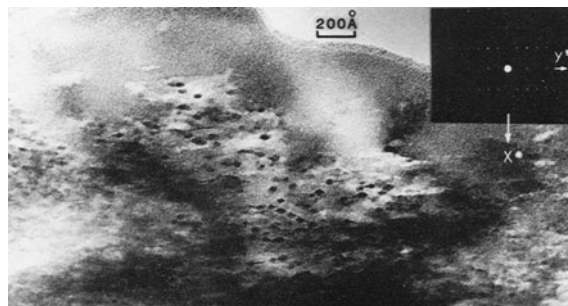


Figure 12. Transmission electron micrograph of early iddingsite in Townsville olivine viewed parallel to Z. Goethite is revealed as small diamond-shaped crystals.

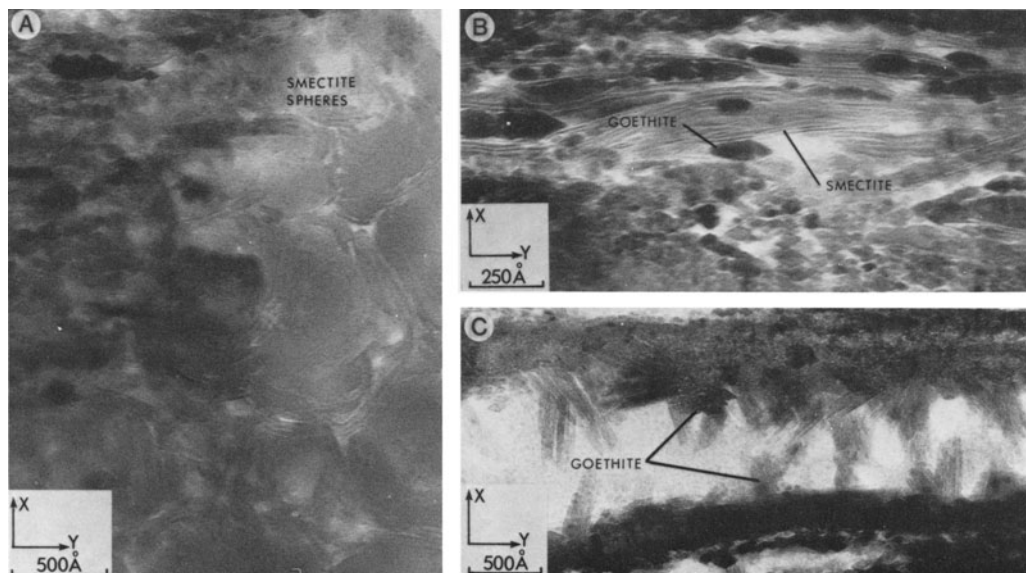


Figure 13. Transmission electron micrographs of later stages of formation of iddingsite in Townsville olivine: (A) goethite crystals and smectite spheres; (B) goethite and planar smectite; (C) goethite crystallized on fissure walls.

TEM scale in botryoidal goethites, identifies them as microcrystals of goethite oriented with their X -, Y -, and Z -axes parallel to X , Y , and Z of olivine, respectively. The phyllosilicate found at this later stage of iddingsite formation in the Townsville olivine may be clusters of spherical crystallites (Figure 13A) or platy crystallites (Figure 13B) oriented approximately parallel to olivine (100). Pseudomorphed olivine crystals

composed largely of goethite are comparatively porous. Some microcrystals of goethite nucleated in fissures and grew in random orientation with respect to the parent olivine (Figure 13C). Continued alteration of the olivine led to an increase in the goethite to phyllosilicate ratio, ultimately producing a goethite pseudomorph constructed of parallel bundles of prismatic (110) microcrystals of goethite about 100 Å in diam-

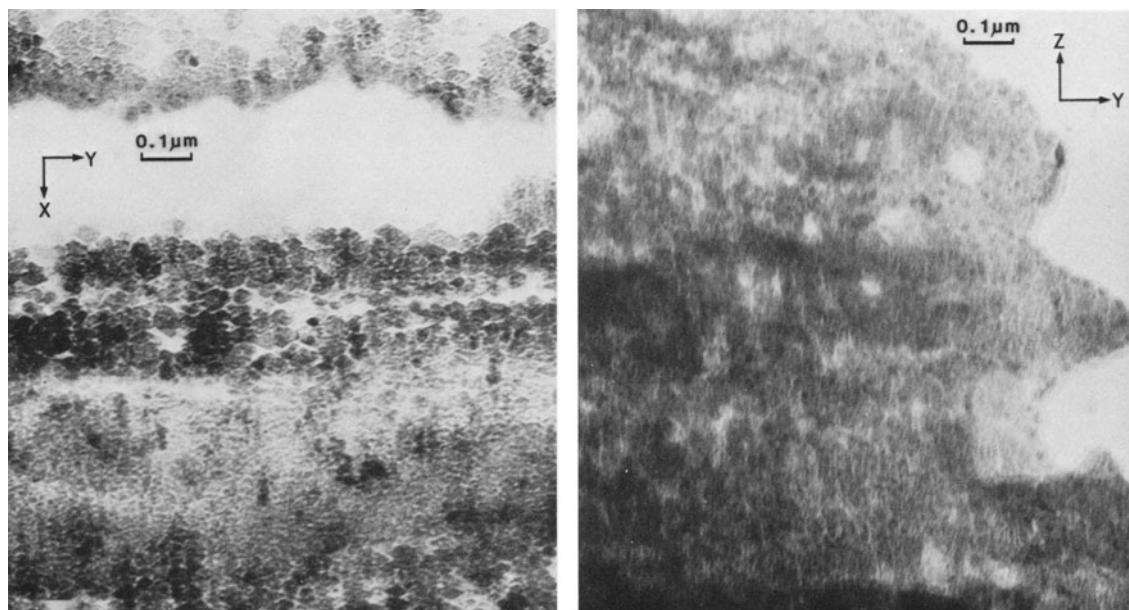


Figure 14. Transmission electron micrographs of goethite after Townsville olivine: (left) viewed parallel to Z ; (right) viewed parallel to X .



Figure 15. Transmission electron micrograph of Baynton olivine alteration associated with oriented inclusions of late magmatic oxides.

eter, as seen in Figure 14. AEM data indicated an Al:Si:Fe ratio for this goethite of 15:4:85, whereas EPMA data for whole pseudomorph gave the ratio 17:8:83.

Alteration associated with planar inclusions. In the earliest stages of weathering of the Baynton olivine, some alteration is associated with planar features that are structurally continuous with (001) of the olivine (Figure 15). Kohlstedt and Vander Sande (1975) observed similar features during a TEM study of natural iron-rich olivines and identified the planar features as lines of iron-rich oxidation products precipitated under magmatic conditions. It is not clear whether alteration during weathering began or terminated at the interfaces between precipitates and olivine. Because the change of structure at the interface should have allowed easier diffusion than might have been possible in a perfect, single-phase, olivine crystal, alteration may have commenced at such interfaces.

Clay-filled fissures. Relatively large, clay-filled fissures were noted in variously oriented sections of all the olivines investigated. They typically range in width from a minimum of about 50 Å, and can have lengths of up to 1 μm. The sides of the fissures are nearly straight and are generally parallel to some identifiable crystallographic plane in the parent olivine. The transition from olivine to clay at fissure boundaries is abrupt. The clay-filled fissures are commonly located in areas

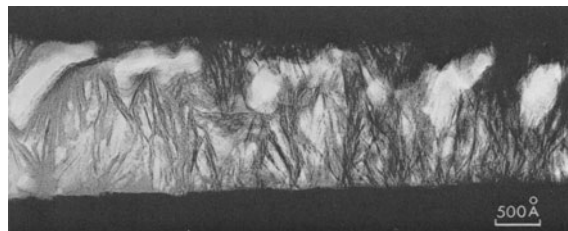


Figure 16. Transmission electron micrograph of smectite-filled channels in Townsville olivine.

of the olivine that are characterized by lamellar alteration zones, but they also occur in areas that appear to be unaltered. As noted above, the clay in these large fissure structures was not damaged by the electron beam to the same extent as the clay bridging the fine 200–500-Å-wide fissures in the lamellar-structured zones.

In the Townsville olivine, the clay in fine fissures in the lamellar alteration zones is commonly oriented such that (001) is perpendicular to the channel walls (Figure 16). In the larger fissures, the strands of clay affixed to the walls usually have this orientation, but away from the walls the clay layers curl and fan. Lattice resolution images show that this clay has a 10-Å basal spacing. Many of the clay layers curve outwards to form hemispherical masses and 'rosettes' (Figure 17) in which the basal spacing is 7 Å. This material, the composition of which is given in Table 2 (analysis e), is shown in the SEM images of fracture and cleavage surfaces of partly altered olivine crystals (Figures 6 and 7).

INTERPRETATION

The three olivines examined in this study have approximately the same composition. Iddingsite alteration progresses inwards from the margins of the crystals by a process that appears to have involved very narrow diffusion pathways. Much of the iddingsite in only slightly altered crystals contains relict olivine, saponite, and minor goethite. With increased weathering, the remaining olivine, and then the smectite, was lost, leaving a very porous oriented aggregate of goethite.

Our field observations, in conjunction with the optical data, support Colman's (1982) view that iddingsite forms under oxidizing conditions. The initial alter-



Figure 17. Transmission electron micrograph of halloysite in channel in Townsville olivine; smectite at channel wall.

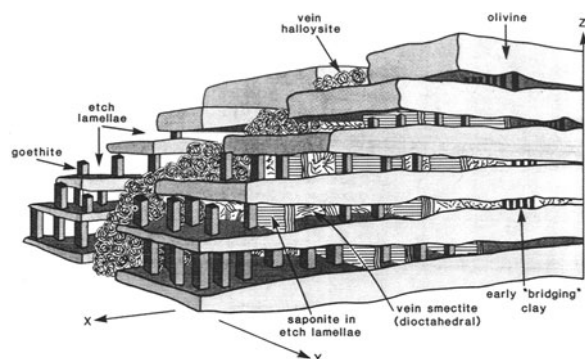


Figure 18. Relationship between various phases and stages of alteration of olivine to iddingsite. Diagram is very much compressed laterally.

ation occurred in lamellar-structured zones in which the olivine was etched along thin planar discontinuities parallel to (001) and spaced at about 200-Å intervals to produce a series of parallel fissures. In general, these zones were formed adjacent to cleavages or fractures. The reason for such regular etching is unknown, but both extrinsic and intrinsic factors may be considered. One possible extrinsic cause is that distortion of the olivine structure at an initial site of dissolution may have produced a series of regular discontinuities which facilitated further dissolution at a certain minimum distance, here, 200 Å. An intrinsic cause may be a fundamental periodic variation in olivine composition with a 200-Å wavelength. Alternatively, the alteration may have been initiated at a lattice misfit between Fe-rich and Mg-rich zones in the parent olivine crystal, for example, at the boundary between core and rim. Olivines containing internal zones of iddingsite were reported by Ildefonse (1983). Lattice misfit between the *X*-axis dimensions of a forsterite-rich core and a fayalite-rich rim might have been accommodated by periodic edge dislocations with Burgers vector $c/2$ spaced at about 240 Å ($80 \times c/2$ for $Fe_{20} = 81 \times c/2$ for Fe_{90}). Diffusion along regularly spaced dislocations could have initiated the observed etched fissures of the lamellar-structured alteration zones.

The opening of fractures and cleavage planes and the associated formation of zones of lamellar fissures were probably related principally to the diffusion of water into the olivine crystals, dissolution and oxidation of components of the structure, and concomitant leaching. The introduction of Al and Na from outside the olivine was important in these early reaction processes, the Al, in particular, providing a basic component with Si, Mg, and Fe for the formation of smectite. The degradation of the olivine structure probably proceeded by dissolution of Mg and its replacement by H^+ , thus distorting the structure and weakening the remaining inter-element bonds. Under these circumstances, Si and Fe likely were released only slowly from the olivine.

In soil materials, the formation of goethite at the expense of hematite is favored by a variety of factors, such as low temperatures, high water activity, low rates of Fe release from parent materials, high organic matter concentrations, and relatively low pH (Schwertmann and Taylor, 1987; Taylor, 1987). In the case at hand, diffusion of oxygen into the microenvironments of the weathering olivine may have been the limiting factor because it would have controlled the formation of the soluble species $Fe(OH)_2^+$ and its dimers and polymers, which Taylor (1987) regarded as precursor nuclei for goethite. Sites adjacent to the etch fissures where the diamond-shaped goethite crystals are seen in (001) projection (Figure 12) might therefore be regarded as zones of relative oxygen enrichment. On the other hand, an apparently close crystallographic control on the distribution of the diamond-shaped crystals seen in parts of Figure 12 may indicate a predisposition for the goethite to have nucleated at particular structural sites in the parent olivine, perhaps dictated by former high Fe concentrations. The high activity of Al in the microenvironments will also have favored goethite formation relative to hematite (Taylor, 1987), although its influence was probably complicated by reactions with Si and other cations leading to the formation of various clay minerals. Early clay minerals formed by reaction of incoming Al and other cations, such as Na and Ca, include dioctahedral smectite of composition $Ca_{0.2}(Al_{0.8}Fe_{1.2})(Si_{3.6}Al_{0.4})O_{10}(OH)_2 \cdot nH_2O$. Later clays, characteristic of fractures and cleavages, include halloysite of composition $(Al_{1.6}Fe_{0.4})Si_2O_5(OH)_4$.

Figure 18 is a diagrammatic representation of the formation of iddingsite and shows the etch fissures present in lamellar-structured zones, the various clay minerals formed in different microenvironments, and the oriented goethite microcrystals. As well as being located in the clay minerals, Al was apparently incorporated both in the goethite microcrystals pseudomorphing olivine and in those growing unconfined from the walls of fissures. Between the fissures in the lamellar-structured alteration zones, additional goethite crystals replaced olivine in an orientation which suggests structural inheritance. Goethite and olivine both have structures based on hexagonal close-packed oxygen arrays (Eggleton, 1984), the metals being coordinated in chains of edge-linked octahedra. More iron may be present in the final iddingsite pseudomorph than was present in the original olivine crystal, as this holds for Al, Ti, and Na. Thus, significant Fe may have diffused into the pseudomorph with these other elements, indicating that the growth of later goethite was epitactic, whereas that of the original diamond-shaped crystals was probably topotactic. On the other hand, the porosity of the iddingsite pseudomorphs may reflect a bulk density that is sufficiently low to indicate that all the Fe is residual, but redistributed into a net-

work of goethite crystallites. As yet, we have no data that distinguish these possibilities. The ultimate product of the weathering transformation, seen in this study only in the Townsville samples, is an olivine pseudomorph composed of highly oriented goethite crystals, each 100 Å wide and 200 Å long. The pseudomorph is aluminous (15 mole %) and contains about 4 mole % Si.

ACKNOWLEDGMENTS

This work was supported by Australian Research Grant Scheme Grant No. E8115611 and a CSIRO/ANU Cooperative Research Grant. The authors thank B. Hyde for the use of the electron microscopes in the Research School of Chemistry at the Australian National University, J. Banfield and J. Fitzgerald for some of the AEM data, the Lunar and Planetary Institute for supporting KS as a Visiting Scientist, and the NASA Johnson Space Center for allowing KS to use their AEM. R. J. Coventry kindly collected the Townsville basalt samples, and R. I. May analyzed them using XRF techniques. We are grateful to H. Zapasnik for thin section preparation, G. G. Riley for XRD data, L. Wittig and R. M. Schuster for drafting, and J. A. Coppi for assistance with photography.

REFERENCES

- Brown, G. and Stephen, I. (1959) A structural study of iddingsite from New South Wales, Australia: *Amer. Mineral.* **44**, 251–259.
- Colman, S. M. (1982) Chemical weathering of basalts and andesites; evidence from weathering rinds: *U.S. Geol. Surv. Prof. Pap.* **1246**, 51 pp.
- Deer, W. A., Howie, R. A., and Zussman, J. (1962) *Rock-forming Minerals. Vol. 1*: Longmans, London, 333 pp.
- Delvigne, J., Bisdom, E. B. A., Sleeman, J., and Stoops, G. (1979) Olivines, their pseudomorphs and secondary products: *Pedologie* **29**, 247–309.
- Eggleton, R. A. (1984) Formation of iddingsite rims on olivine: A transmission electron microscope study: *Clays & Clay Minerals* **32**, 1–11.
- Eggleton, R. A., Foudoulis, C., and Varkevisser, D. (1987) Weathering of basalt. Changes in rock chemistry and mineralogy: *Clays & Clay Minerals* **35**, 161–169.
- Eggleton, R. A. and Smith, K. L. (1983) Silicate alteration mechanisms: *Sci. Geol. Mem. Strasbourg* **71**, 45–53.
- Gay, P. and Le Maitre, R. W. (1961) Some observations on iddingsite: *Amer. Mineral.* **46**, 92–111.
- Ildefonse, P. (1983) Alterations pré-météorique et météorique des olivines du basalte de Belbex (Cantal, France): *Sci. Geol. Mem. Strasbourg* **72**, 69–79.
- Kohlstedt, D. L. and Vander Sande, J. B. (1975) An electron microscopy study of naturally occurring oxidation produced precipitates: *Contrib. Mineral. Petrol.* **53**, 13–24.
- Schwertmann, U. and Taylor, R. M. (1987) Iron oxides: in *Minerals in Soil Environments*, 2nd. ed., J. B. Dixon and S. B. Weed, eds., Ch. 9, Soil Sci. Soc. Amer., Madison, Wisconsin, (in press).
- Smith, K. L. and Eggleton, R. A. (1983) Botryoidal goethite: A transmission electron microscope study. *Clays & Clay Minerals* **31**, 392–396.
- Taylor, R. M. (1987) Non-silicate oxides and hydroxides: in *The Chemistry of Clays and Clay Minerals*, A. C. D. Newman, ed., Mineralogical Soc. Monograph, Longmans, London, 129–202.
- Wilshire, H. G. (1958) Alteration of olivine and orthopyroxene in basic lavas and shallow intrusions: *Amer. Mineral.* **43**, 120–147.
- Wilson, R. E. (1978) Mineralogy, petrology and geochemistry of basalt weathering: B.Sc. (H) thesis, LaTrobe University, Melbourne, Australia, 55 pp.

(Received 7 October 1985; accepted 4 June 1987; Ms. 1527)